13 Detection of Land Surface Temperature in the Northwest Part of Bangladesh

A Remote Sensing Based Approach

Arshib Imtiaj, Md Hasibul Hasan, Md. Mostafizur Rahman, Md. Salah Uddin, and Saeid Eslamian

13.1 INTRODUCTION

Urban areas are now the preferable living place for about half of the world's population, this is expected to reach two-thirds by 2030 (Zhang, 2016). The increasing statistics of global urbanization have had an adverse effect on the micro climate due to the rise in air and surface temperatures (Makvandi et al., 2019; Souza et al., 2016). All over the world, this land use land cover (LULC) change, especially vegetation, is improvised by impervious cover, for instance, concrete buildings, pavements, or asphalt (Makvandi et al., 2019; Fathian et al., 2015). This results in energy absorption and radiation that may accelerate local and global problems such as biological hazards (air pollution and urban heat islands), concentration of greenhouse gases, and deterioration of public health and wellbeing (Lai and Cheng, 2010). However, the increasing temperature of urban areas in the modern era is a burning issue in many developed and underdeveloped countries. Cities such as London (UK), Bolzano (Italy), Madrid (Spain), and Nice (France) in Europe (dos Santos, 2020; Hellings and Rienow, 2021); Kumasi (Ghana) and Freetown (Sierra Leone) in Africa (Buo et al., 2021; Mustafa et al., 2021); and Tokyo (Japan), Beijing (China), Delhi (India), Mumbai (India), and Kuala Lumpur (Malaysia) in Asia (Dutta et al., 2019; Hua and Ping, 2018; Jain et al., 2021; Liu et al., 2021; Siddique et al., 2020) are being affected rigorously by land surface temperatures. Also, in less developed nations such as Bangladesh, the effect is not negligible, particularly in the mega-city of Dhaka.

According to WB (2013), "Bangladesh will be the most affected country in South Asia by an expected 2°C rise in the world's average temperatures in the next decades, with rising sea levels and more extreme heat" (Mirza, 2011). On the other hand, northern parts of Bangladesh have been facing drought problems and a reduction in water bodies (Hoque et al., 2020). Past experience has revealed that the northwestern part of Bangladesh has gone through critical changes such as landscape degradation, river erosion, land use changes, and extensive unplanned human activities (Kafy et al., 2021b; Mim and Zamil, 2020). Besides, quick urbanization in recent decades has attracted people to migrate to this area, with the city Rajshahi no exception (Kafy et al., 2020; Rahman, 2010) as it is one of the warmest regions in northwestern Bangladesh because of its geographical location and socioeconomic conditions. This massive rate of haphazard infrastructural development with its construction materials is affecting the urban climate, which is influencing district temperature rise (Dewan et al., 2021). This is due to the rural–urban migration from the nearby disaster-prone areas (river erosion, flood, and drought). Nowadays migrants prefer Rajshahi rather than Dhaka because of its low cost of living, employment opportunities, and available municipal services (Hasan et al.,

DOI: 10.1201/9781003473398-16

2017; Hasan et al., 2022; Rahaman et al., 2021). As a result, vegetation and water reserves are gradually reduced with the increase of settlements (Kafy et al., 2021a, 2021b).

During the last decade, several research studies regarding LST detention have been conducted, however, most of the studies were Dhaka-based (Ahmed et al., 2013; Imran et al., 2021). Several early studies have addressed land surface temperature and urban heat islands (Roy et al., 2021). However, little importance has been given to the capture sensitivity analysis and the most responsible factors behind the change in land surface temperature (Ferdous and Rahman, 2018) in the northwestern part of Bangladesh. Besides, temperature mapping with a physical survey is relatively expensive, whereas the use of remote sensing (RS) and geographic information systems (GIS) methods in land temperature detection are being used a lot by researchers for their simplicity and cost-effectiveness (Dey et al., 2021; Habibie et al., 2021).

This chapter will deal with investigating the relationship between land surface temperature variations over land cover by using the normalized difference vegetation index (NDVI), normalized difference water index (NDWI), and normalized difference built-up index (NDBI) techniques to identify the comfort zones within the study area. In addition, a comprehensive assessment of sensitivity has been carried out to explore which component is more sensitive to heat. The approach of remote sensing along with GIS has been followed in bringing up the scenario where satellite images (Landsat-5 TM and Landsat 8 OLI) from different years (1995, 2005, and 2019) were used. The findings thus provide a guide to the concerned authorities in the development policies for better land zoning ways of alleviating warming effects.

13.2 STUDY AREA

Rajshahi district is predominantly an agricultural area (BBS, 2011) and is well-known throughout Bangladesh as an educational city. It is located between the latitudes of 24°07′ and 24°43′ north and the longitudes of 88°17′ and 88°58′ east. The district's total area is 2,425.37 km^2, with a total of 633,758 houses and 2,595,197 people (BBS, 2011) This district is bordered on the north by Naogaon, on the south by the Padma River and Kushtia district, on the east by Natore, and on the west by Chapainawabganj, while Rajshahi City Corporation (RCC) is located on the banks of the Padma River (Figure 13.1).

The main sources of income are agriculture (59.35%), non-agricultural laborers (3.36%), industry (0.99%), commerce (14.25%), transportation and communication (4.36%), service (8.97%), construction (1.45%), and others (6.74%) (BBS, 2011). Although the district is not industrially developed, it has experienced a significant increase in unplanned housing activity in recent years. RCC is presently provoked by several commercial activities such as expanding market areas, rapidly developing restaurant businesses, and so on, which are impacting the urban land use activity. As a result of the increased construction rate to accommodate this high demand, the city is losing its green spaces. The climate in Rajshahi is classed as tropical, where the summer is much rainier than the winter (BBS, 2011). During the winter season, the minimum and maximum mean temperatures range from 9°C to 14°C. The minimum and highest mean temperatures in the summer range from 25.5°C to 38.7°C. In April, the humidity level was around 77%, and in July, it was over 88% (BBS, 2011).

13.3 METHODOLOGY

A systematic approach was adopted to prepare the LULC map from satellite images and analyze the sensitivity with different indices. First, this study processed satellite images through an image processing system where the radiometric and geometric corrections were used. The supervised classification technique was adopted for the LULC map which needs prior to accuracy assessment, to check whether the result is acceptable or not. This study also considered three different normalized indices to understand the land use and land cover scenario. To calculate the land surface temperature, three different steps namely, conversion of the digital number (DN) values to spectral radiance,

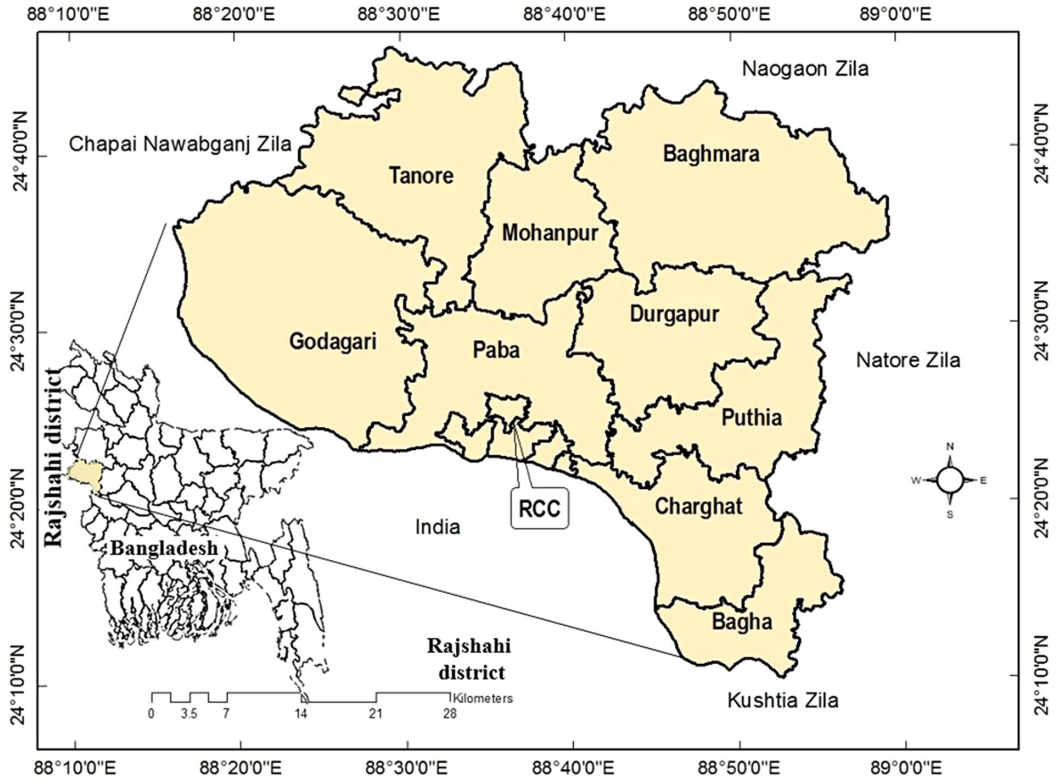

FIGURE 13.1 Study area map.

then spectral radiance to top of atmosphere (TOA) brightness temperature, and land surface emissivity (LSE) were used (Figure 13.2).

13.3.1 Remote Sensing Data

The satellite images were acquired from the United States Geological Survey (USGS) with a 30 m resolution and had cloud coverage of less than 10%. Landsat 5 TM and Landsat-8 OLI-TIRS images were considered for the years of 1990, 2006, and 2018 respectively that were taken by using 138/43 path and row (Table 13.1).

13.3.2 Image Pre-preprocessing

Both geometric and radiometric corrections have been conducted to process the satellite images for further analysis. The geometric correction is confined to the process of geo-referencing of Landsat images with the Universal Transverse Mercator (UTM) projection system that was ratified by availing some known ground points. In this study, 25 ground points were identified from Google Earth to transfer images into the Bangladesh Transverse Mercator (BTM) map projection system, having the datum of D_Everest_1830 from the World Geodetic System (WGS84).

On the other hand, the reflectance sensor data is influenced by many factors (e.g., atmospheric absorption and scattering, in-sensor factors, data processing procedures, etc.) (Teillet, 1986). Moreover, these effects need to be addressed to avoid the task becoming complicated (Mas, 1999; Turker and Asik, 2002). A radiometric correction needs to capture the absolute surface reflectance digital number (DNs) generated from the satellite (Chavez, 1996). The study followed (López et al., 2016) for the radiometric correction of the satellite images.

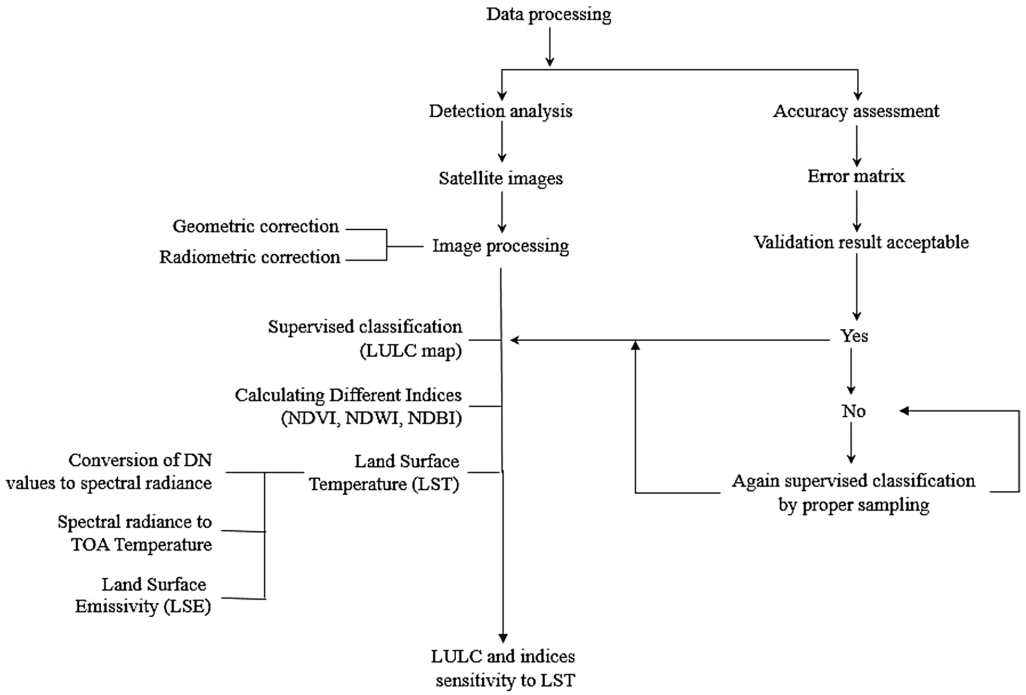

FIGURE 13.2 Flow chart of the data analysis.

TABLE 13.1
Details on Collected Satellite Image

Sensors name	Date of data acquired (yy-mm-dd)	Time	Path	Row
Landsat 4–5 Thematic Mapper (TM)	1995-04-18	03:39:25 PM	138	43
Landsat 4–5 Thematic Mapper (TM)	2005-04-13	04:17:43 PM	138	43
Landsat 8 Operational Land Imager (OLI)	2016-04-11	04:30:12	138	43

13.3.3 Calculating Different Indices

The study considered three different normalized indices to understand the land use and land cover scenario of the study area. These are the normalized difference vegetation index (NDVI), normalized difference water index (NDWI), and normalized difference built-up index (NDBI) respectively. NDVI is the most commonly used vegetation index to indicate a plant's photosynthetic activity. On the other hand, NDWI and NDBI show water bodies and built-up areas accordingly. These three indices were calculated by using Equations (13.1), (13.2), and (13.3) given below (NASA, 2015):

$$NDVI = \left(NIR - Red\right) / \left(NIR + Red\right) \tag{13.1}$$

$$NDWI = \left(Green - NIR\right) / \left(Green + NIR\right) \tag{13.2}$$

$$NDBI = \left(SWIR1 - NIR\right) / \left(SWIR + NIR\right) \tag{13.3}$$

Where, bands 3, 4, 5, and 6 are green, red, NIR, and SWIR1 for Landsat 8 OLI, similarly bands 4 and 3 are NIR and red for Landsat TM 4-5.

13.3.4 Deriving Land Surface Temperature (LST)

To detect land surface temperature, calculating the digital number (DN) into the top of atmosphere (TOA) brightness temperature is essential, followed by the conversion of TOA brightness temperature into land surface temperature.

13.3.4.1 Conversion of DN Values to Spectral Radiance

LST is calculated from the thermal band where bands 10 and 11 are the thermal bands for Landsat 8 and band 6 is the thermal band for Landsat TM 4-5. The digital numbers (DNs) of bands 6, 10, and 11 were converted to spectral radiance using the Equations (13.4) and (13.5) given below: (NASA, 2015)

$$L_{\lambda} = M_L.Q_{cal} + A_L \quad \text{(For Landsat 8 OLI)} \tag{13.4}$$

$$L_{\lambda} = \frac{V}{225\left(R_{max} - R_{min}\right) + R_{min}} \quad \text{(For Landsat TM 4-5)} \tag{13.5}$$

Where L_{λ} = Spectral radiance; M_L = Radiance multiplicative scaling factor for the band; A_L = Radiance additive scaling factor for the band; and Q_{cal} = pixel value of band 10 and 11 in DN. Similarly, V represents the DN of band 6; R_{max}, 1.896(mW×cm−2×sr−1) and R_{min}, 0.1534(mW×cm−2×sr−1).

13.3.4.2 Spectral Radiance to TOA Temperature

Then spectral radiance of bands 10 and 11 of Landsat 8 and band 6 of Landsat TM 4-5 were converted to top of atmosphere (TOA) brightness temperature where TOA was converted to degrees Celsius as it was derived in kelvin. The formula is shown below: (NASA, 2015)

$$BT = \frac{K_2}{L_{\lambda}\left\{\left(\frac{K_1}{L_{\lambda}}\right)+1\right\}} \tag{13.6}$$

Where, BT refers to top of atmosphere brightness temperature, in Kelvin; L_{λ} = Spectral radiance; $K1$ = Thermal conversion constant for the band; and $K2$ = Thermal conversion constant for the band.

13.3.4.3 Calculate Land Surface Temperature

To investigate LST, the value of land surface emissivity (LSE) is needed along with TOA temperature. The LST and LSE of Landsat 8 OLI and Landsat TM 4-5 can be calculated by the following formula (Weng et al., 2004):

$$P_v = [(NDVI - NDVI_{min}) / \left(NDVI_{max} - NDVI_{min}\right)]^2 \tag{13.7}$$

$$e = 0.004\ P_v + 0.986 \tag{13.8}$$

$$LST = BT / 1 + \lambda * \left(BT / p\right) * ln\left(e\right) \tag{13.9}$$

Where, e = Land surface emissivity; P_v = Proportion of vegetation; λ = wavelength of emitted radiance; P = h*c/s (1.438*10^{-2} m K); h = Planck's constant (6.626×10^{-34} J s); s = Boltzmann Constant (1.38 ×10^{-23} J/K) and c = Velocity of Light (3 ×10^{8} m/s).

TABLE 13.2
Land Cover Types

Land cover type	Description
Built-up Area	Mainly all infrastructure. Such as residential, commercial, mixed-use, and industrial areas, settlements, road networks, pavements, etc.
Water Body	Ponds, wetlands, marshy land, low land, and swamps.
Vegetation	Trees, natural vegetation, mixed forest, gardens, parks, and playgrounds.
Agricultural	Agricultural lands, vacant land, open space, and crop fields,

13.3.5 Land Cover Classification

There are various types of classification methods available to identify the LULC status from RS data. Broadly, the methods are supervised and unsupervised classification approaches. The unsupervised classification method is based on the iterative self-organizing data analysis technique algorithm (Lu et al., 2004). On the other hand, supervised classification is based on training sample analysis, which is decided by researchers/experts, and this type of classification method is more precise compared to others to see the accuracy obtained by the MLC method. Considering this benefit, the supervised classification method is the most popular and most widely used by many researchers (Fonji and Taff, 2014; Islam et al., 2015, 2018; Islam and Sarker, 2016). Having this consideration, the study used supervised classification with the maximum likelihood classification (MLC) algorithm for LULC determination by using ArcGIS 10.3 software. The types of LULC found from the analysis are listed in Table 13.2.

Initially, the corrected images (geometric and radiometric corrected) of each date are compiled into a single layer using three bands to create a false color composite (FCC) image to distinguish different LULC types like agricultural land, vegetation, and settlement.

13.3.6 Error Matrix

The error matrix is one of the best ways to assess the accuracy of satellite images for land use land cover analysis as it aims to assess the effectiveness of sampling for land cover classification (Hasan et al., 2020; Hasan et al., 2023; Rwanga and Ndambuki, 2017). For the error matrix, a satellite image of April 2019 has been selected where 160 ground points were chosen. Google Earth was used as a reference source for ground truthing. Table 13.3 presents the error matrix of the land cover classified image of 2019 that shows the relationship between ground truth data and the corresponding classified data. The columns of the table represent produced value (map makers' point-of-view, selecting a sample for the land cover) and the rows express observed value (user's point-of-view, how accurately land class is presented on the ground). For accuracy assessment, the study considered the producer's and user's accuracy, commission, and omission errors, overall accuracy, and Kappa coefficient followed by (Rwanga and Ndambuki, 2017) that have been derived from the error matrix.

13.4 RESULTS

13.4.1 Accuracy of the Study

The land covers derived from the analysis and the land covers from Google Earth are well-matched with better accuracy. The result shows that the producer Accuracy (PA) ranged from 100% to 0.63% whereas the user accuracy (UA) was found at 98% to 80% (Table 13.4). Water bodies and vegetation

TABLE 13.3
Error Matrix

Land use class	Water body	Built up area	Agricultural land	Vegetation	Row total
Water body	40	0	1	0	41
Build up area	0	40	10	0	50
Agricultural land	0	0	25	3	28
Vegetation	0	0	4	37	41
Column Total	40	40	40	40	160

TABLE 13.4
Accuracy Assessment

Land class	UA	PA	CE	OE	OA	Kappa
Water body	0.98	1	0.02	0	0.89	0.85
Built up area	0.80	1	0.20	0		
Agricultural land	0.89	0.63	0.11	0.37		
Vegetation	0.90	0.93	0.10	0.08		

are found to be more accurate both for PA and UA. High commission error (CE) in this study is found for built-up areas (20%) and high omission error (OE) for agriculture (37%). That means that overestimation was incorrectly included for the built-up area while sampling, on the other hand, underestimation was evaluated for agricultural land cover. Besides, overall accuracy is found at 89% and the Kappa coefficient is measured at 0.85 that illustrates preferable accuracy for each land cover classification in its field of interest according to Fleiss et al. (2004) (Fleiss et al., 2004).

13.4.2 Temperature Difference between Urban and Rural Areas

RCC is considered an urban area, whereas the other 9 Upazilas are supposed to be rural areas. These classifications have been done on the basis of some criteria (e.g., land cover type, population size, and municipality services). The temperature difference between urban and rural areas is identified in the study area due to their land cover differences. For instance, the amount of concrete and bitumen and the existence of greenery and water bodies. The maximum land cover of the urban area is the built-up area where a plethora of vegetation, agricultural land, or water bodies are found in the rural part of Rajshahi or vice versa.

Figure 13.3 illustrates that the temperature difference between urban and rural areas varies by 1° to 2° for each type of land cover, where for every land class, the rural area temperature is lower than the urban due to the absorption of heat by built-up areas. More specifically, the mean temperature in built-up areas is 31.87°C and in rural areas it is 32.82°C. Similarly, the mean temperatures are 30.39°C and 31.35°C for vegetation, 29.90°C and 31.61°C for agricultural land, as well as 29.77°C and 30.89°C for aquatic land.

From Figure 13.4, it has been found that the southern and southwestern parts of the urban area are concentrated on built-up areas, and the northern and northeastern parts are covered by other land use types (Figure 13.4, A2). On the other hand, high temperatures have been observed in the southern and southwestern areas and lower temperatures in other parts of the city (Figure 13.4, A1). Consequently, a proportionate relationship exists between surface temperature and LULC. Likewise, Godagari, Paba, Durgapur, Puthia, and Charghat Upazilar rural areas seem to be hotter

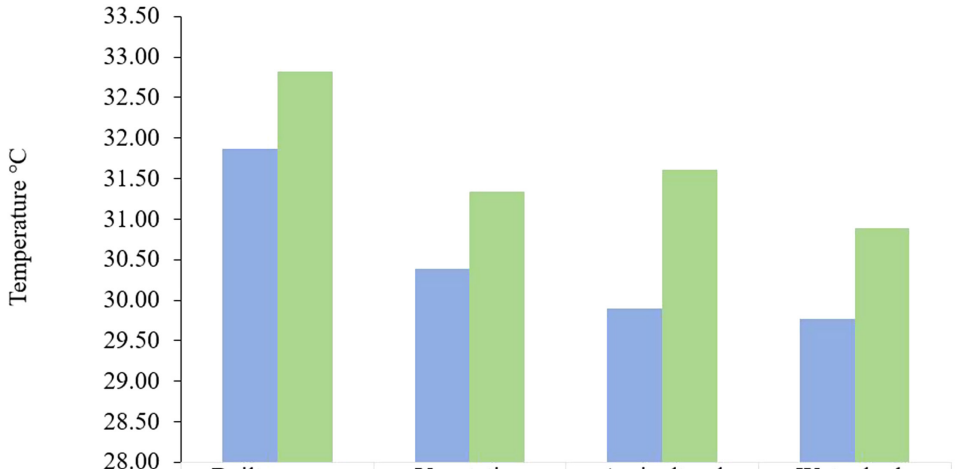

FIGURE 13.3 LULC-wise temperature difference between urban and rural areas in 2019.

than the other Upazilas (Figure 13.4, B2) where there is a corresponding relationship between surface temperature and LULC as in urban areas (Figure 13.4, B1).

13.4.3 Analysis of Comfort Zone

The temperature variation from 1995 to 2019 has been identified both for urban (RCC) and rural (Other Upazilas except RCC) areas to understand the comfort zone (Brändle et al., 2015). To do that, temperatures are divided into four classes, where temperatures up to 15°C are considered a cool area, 16–25°C as a comfort zone, 26–32°C are treated as warm, and more than 32°C as an uncomfortable area. This study found that the temperature values ranged from 23°C to 40°C. Figure 13.5 illustrates that maximum areas of Rajshahi district are in the warm zone all over the study period, having no cool zone. A small portion of a comfortable zone was found in Baghmara Upazila in 1995, whereas most of the areas of Tanore, Godagari, Paba, and Charghat were found to be uncomfortable areas until 2005. But in the year 2019, the spatial distribution of comfort zones showed a reduction in uncomfortable hot zones whereas Rajshahi City Corporation gave the inverse result.

Table 13.5 illustrates that the warm zone decreased by 88.57 km^2 in 2005 and again increased to 200.15 km^2 in 2019. However, the area of comfort zone was in a decreasing trend all over the study period, which decreased to 0.84 km^2 in 2005 and no comfort zone was available in the year of 2019. Though the very hot zones decreased in 2019, RCC followed a reverse trend in this case.

13.4.4 Relation between LST and Different Indices

Figure 13.6 shows the temperature difference between various Upazilas of Rajshahi in the year 2019, where the highest minimum temperature was found in Rajshahi City Corporation and the lowest in Puthia. Figure 13.7 shows that Rajshahi City Corporation, treated as an urban area, is found built-up concentrated (395.001 km^2) where a small amount of agricultural and vegetated areas, as well as water bodies, are available. Besides, a large amount of agricultural land is found in Godagari, Tanore, Mohonpur, and Baghmara Upazila, where the maximum vegetation is in Bagha Upazila.

NDVI's highest value varies from 0.74 to –0.19, whereas NDWI and NDBI vary from 0.65 to –0.33 and 0.33 to –0.74. The NDVI value is found high in several areas (e.g., Mohanpur, Baghmara,

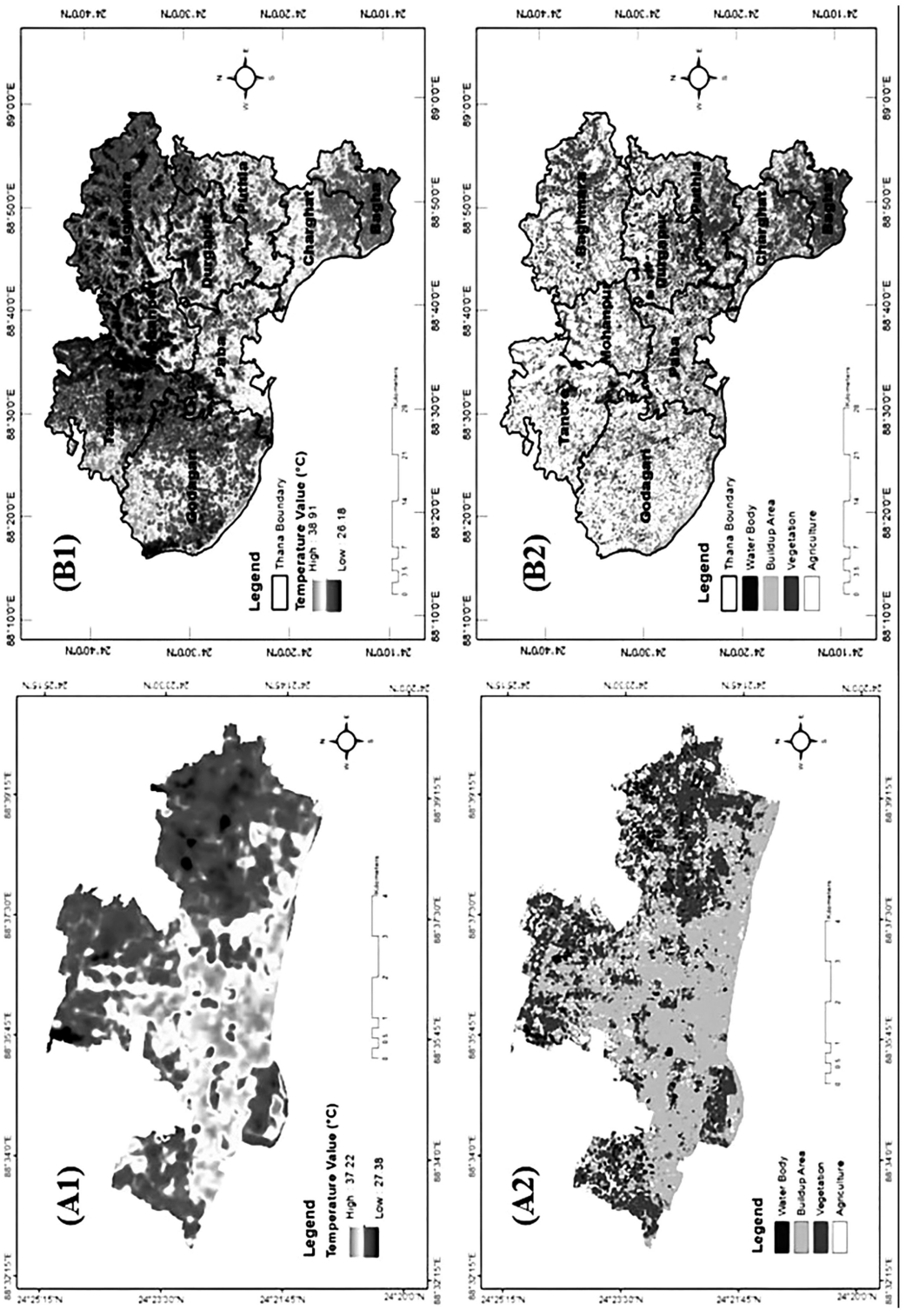

FIGURE 13.4 LST and land cover of urban and rural area, (A1) LST of urban area, (A2) Land cover of urban area, (B1) LST of rural area, (B2) Land cover of rural area.

FIGURE 13.5 Year-wise comfort zone scenario of Rajshahi district, (A) 1995, (B) 2005, (C) 2019.

TABLE 13.5
Area Distribution in km² of Comfort Zone of Rajshahi District in 1995, 2005, and 2019

Temperature category	Area (km²), 1995	Area (km²), 2005	Area (km²), 2019
Cool	–	–	–
Comfortable	6.15	0.84	–
Warm	1684.16	1595.59	1793.74
Uncomfortably hot	509.39	603.28	405.97

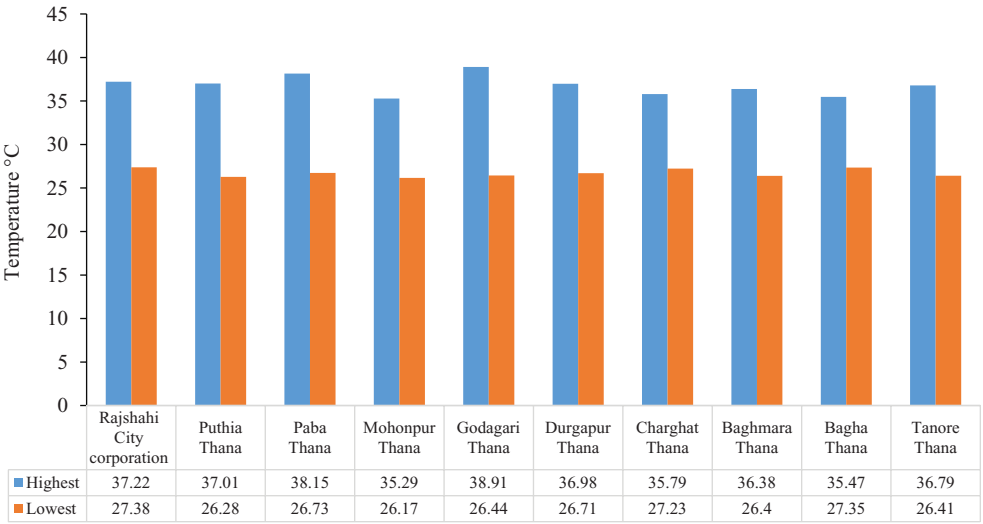

FIGURE 13.6 Highest and lowest temperature difference of different upazila of Rajshahi district in 2019.

Tanore, Godagari Upazila) having low temperatures. Similarly, RCC and Godagari Upazila fall under lower NDWI values with higher temperatures. With the increase in NDWI value, the presence of water bodies increases and temperature decreases, as well as NDVI (with respect to vegetation). On the other hand, with respect to NDBI, RCC, and the adjacent areas of Paba, Puthia, and Charghat that are close to the city corporation area, the northwest portion of Godagari and Tanor are found to have high values of NDBI and temperature.

13.4.5 Indices Sensitivity to Temperature

A simple application of the correlation coefficient can be exemplified by using data from a sample of 348 points that were selected from different places in the RCC shown in Figure 13.8. All of the indices (e.g. NDVI, NDWI, and NDBI) are continuous and skewed with the response to temperature. From Pearson correlation analysis between indices and LST, the resulting correlation coefficients are –0.80 (NDVI), –0.88 (NDWI), and 0.88 (NDBI) respectively. In this case, all of the indices are strongly correlated with temperature, i.e., high positive and negative correlation. Where two indices (NDVI and NDWI) correlation coefficients are similar and lead to the same conclusion, the NDBI reveals different statistical conclusions. According to Hinkle et al. (2003), the correlation coefficient between 0.70 to 0.90 or –0.70 to –0.90 has a high positive or negative correlation where the above

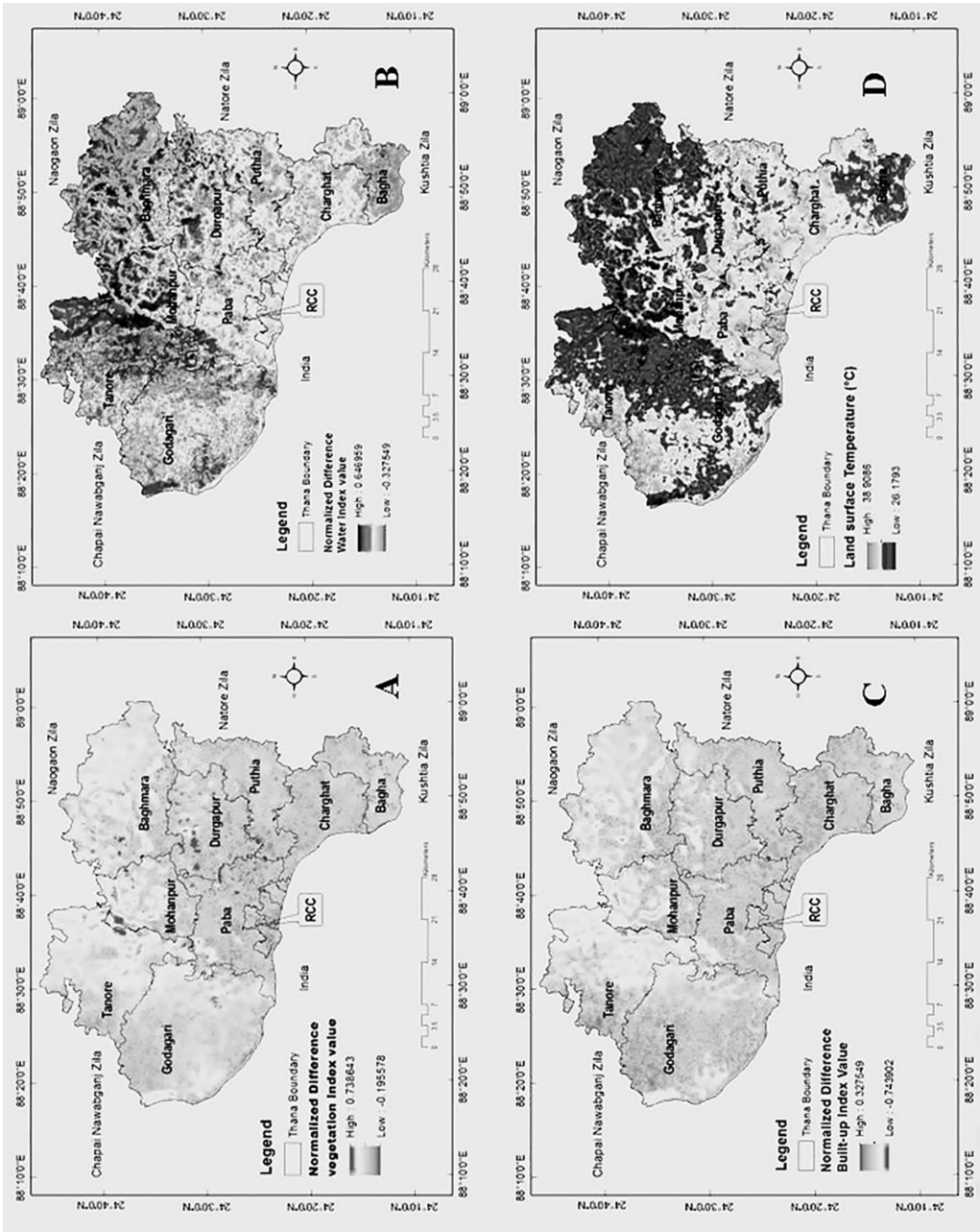

FIGURE 13.7 Indices comparison with LST, (A) NDVI, (B) NDWI, (C) NDBI, and (D) LST.

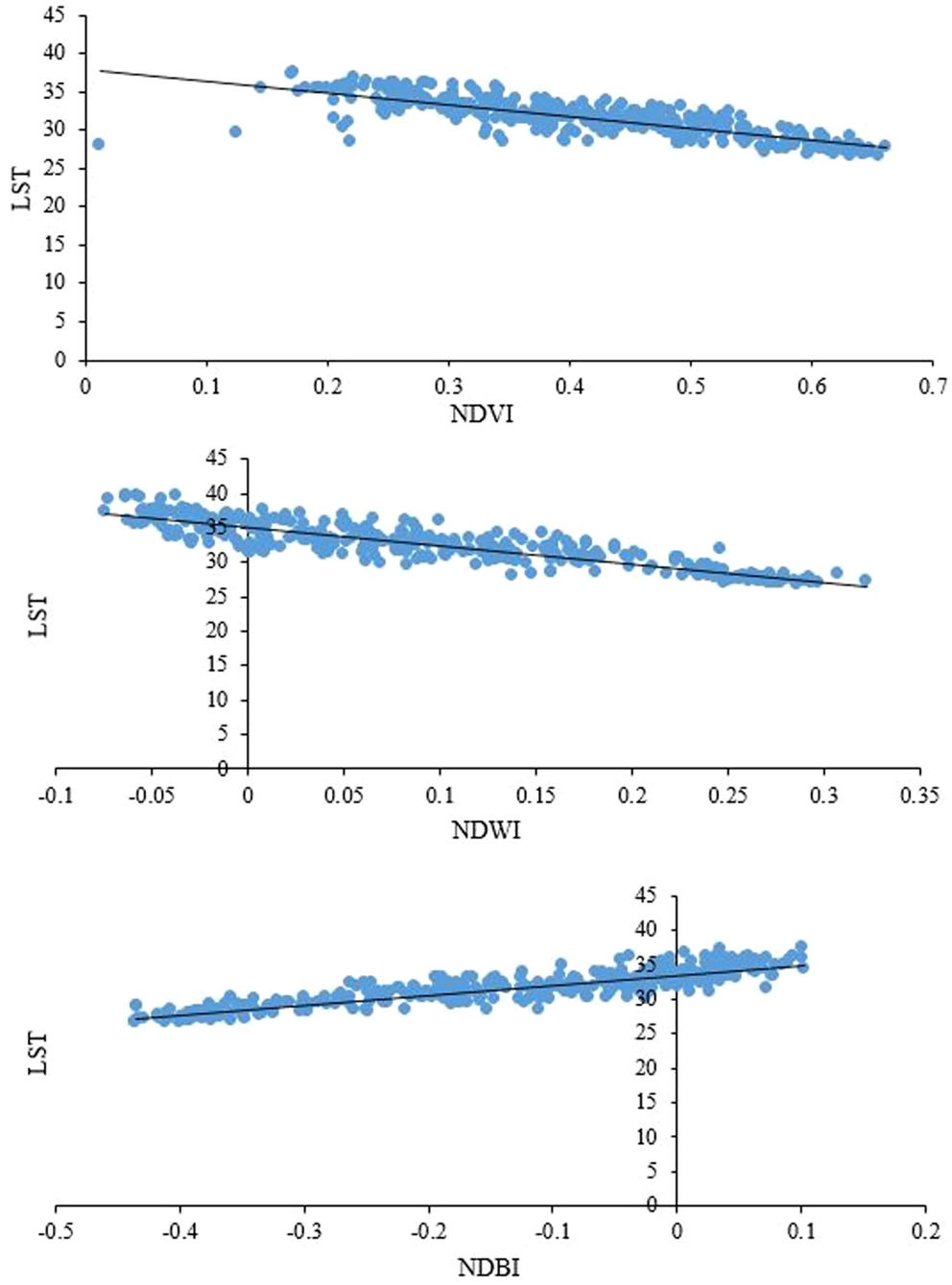

FIGURE 13.8 Correlation coefficient analysis between LST and three different indices (NDVI, NDWI, and NDBI).

or below value range demonstrates a very high or moderate correlation. In this study, the correlation coefficient value between NDWI, NDVI, and temperature was found to be –0.81 and –0.88 respectively, which depict a highly negative correlation. On the contrary, the NDBI value is found at 0.88, which means it is highly positively correlated with temperature. Therefore, with an increase in the NDBI value, temperature increases, and with a decrease in the NDBI value, temperature decreases. Reverse situations have been found in the case of NDWI and NDVI.

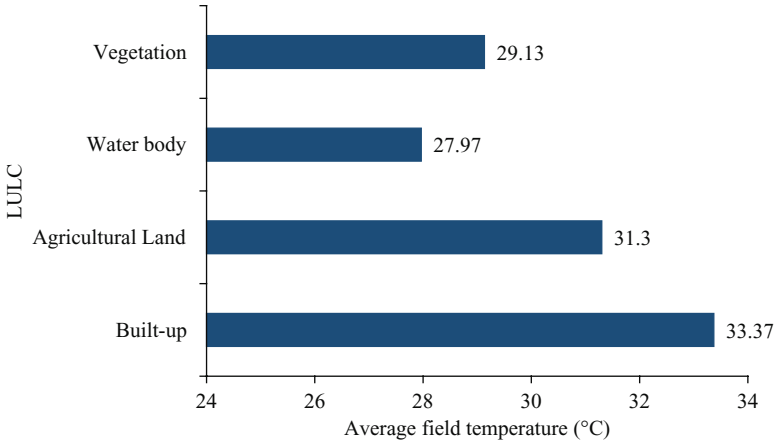

FIGURE 13.9 Average field temperature of the study area.

To understand the above relationship, a field survey was conducted in RCC on the different land covers to cross-check the sensitivity to temperature. Figure 13.9 shows the temperature value for four different land covers where built-up areas have the highest value (33.37°C). On the other hand, the value is 29.13°C for vegetation, 27.97°C for water bodies, and 31.30°C for agricultural land.

13.5 DISCUSSIONS

The study was carried out to determine the consequences of land cover changes on land surface temperature in Rajshahi district for the year 2019. Furthermore, chronological changes in temperature have been found in the years 1995, 2005, and 2019. Previous studies regarding LULC and LST (Ahmed et al., 2013; Imran et al., 2021; John et al., 2020; Kafy et al., 2020; Raja, 2012) were helpful in leading as well as comparing the results of the study. High temperatures in built-up areas, and contrariwise sloping temperatures in agriculture, vegetation, and water bodies have been fabricated in this study, which coincides with previous research (Ahmed et al., 2013; Imran et al., 2021; John et al., 2020). Dey et al. (2021) reported that in Rajshahi district, the buildup area has increased by 14.78% while greenery space has decreased by about 6.27% since 1990. Kafy et al. (2021b) added that about 3.35 % of the area in Rajshahi will be more than 35°C due to the conversion of urban areas by 2039. Nevertheless, the study results show that 18% (396 km^2) of the study area was built-up areas in 2019, among which almost 50% of the built-up area was in RCC. These concrete-concentrated urban areas led to the increase in LST, while Imran et al. (2021) revealed similar results in Dhaka, Bangladesh.

The southern part of Rajshahi (especially the RCC area) experienced substantial growth in settlement areas, leading to the LST. Urban expansion occurred due to population growth in Rajshahi city due to a higher birth rate and migrated people from rural areas to urban areas for the sake of better livelihood (Kafy et al., 2021c, 2021d). Sometimes this is due to natural or anthropogenic disasters (river erosion, flood, drought, scarcity of employment, etc.). As Kafy et al. (2021a) argued, most of the water bodies and greenery turned into settlements from 1990 to 2019.

On the other hand, with respect to the comfort zone of Rajshahi, the uncomfortable zone was decreased by about 4.70%, though the warm area was increasing at an alarming rate (9.06%) from 1995 to 2019 (Figure 13.10). The study also found that the number of comfortable zones (between 15–25°C) decreased by 0.3% where RCC (urban areas) gradually turned into warm to uncomfortably hot areas. A corresponding trend of temperature shifting was identified by Imran et al. (2021) in Dhaka city of Bangladesh where the temperature increased by 0.24°C per year, while Pal and Ziaul (2017) found an increase of 0.11°C per year in West Bengal, India.

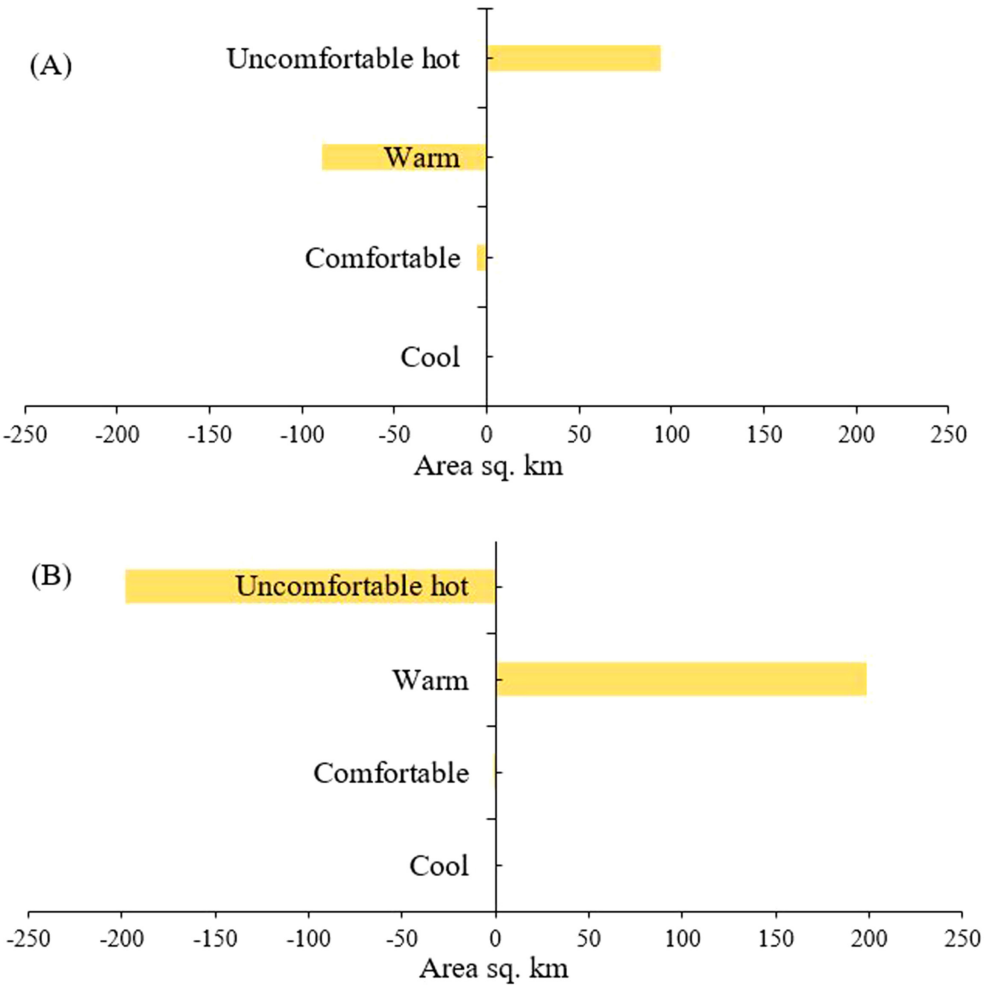

FIGURE 13.10 Gain and loss of comfort zone (A) 1995 to 2005 and (B) 2005 to 2019.

Further, regression analysis of the study resulted in a positive accordance between LST and NDBI but a negative kinship between LST and the other two indices (NDVI and NDWI). The analysis shows that LST increased with the increase in built-up areas (NDBI) or vice-versa. On the other hand, LST decreased when vegetation (NDVI) and water bodies (NDWI) increased in trend or vice-versa. Likewise, Imran et al. (2021) identified similar results from the perspective of LST and different land cover indices that testify to the LST sensitivity to indices.

The findings of this chapter thus suggest that urbanization is the forward driver for LULC and LST respectively. However, without pledging a better decentralization policy, it is hard to control the unplanned built-up areas in Rajshahi because they gradually increase their major opportunities and services (e.g., education, medical facilities, jobs) (Farhana and Mannan, 2018).

13.6 CONCLUSIONS

The study reveals the relationship between the land cover and surface temperature in the Rajshahi district of Bangladesh, where the temperature difference between the concrete concentrated (urban) and agriculture, vegetation, and water concentrated (rural) has been clearly identified. This relationship is further clearly identified by linear regression analysis between different indices of NDVI,

NDWI, NDBI, and LST. The temperature difference between the urban and rural areas is almost 1°C to 2°C. Most of the land in the urban area is wrapped in rock or asphalt, and these construction materials are the main reasons for increasing urban temperature, especially in RCC. However, the highest temperature difference between the urban and rural areas was found in the agricultural land (1.71°C), where 1.01°C in the built-up area, 0.98°C in vegetation, and 1.12°C in the water body. Besides, to find a comfortable zone, it is notable that the hot zone (15°C to 25°C) has been on an increasing trend from 1995 to 2019, irrespective of LULC. It is partially supposed to be the reason for LST due to climate change, though further research ought to be needed to confirm it. From the findings of the study, policymakers in Rajshahi ought to be concerned about urbanization and future urban growth. An environmentally friendly proper guideline is thus needed both for horizontal and vertical expansion where green roofs, climate-friendly construction materials, and extensive tree plantation may reduce the urban microclimate warming effect.

ACKNOWLEDGMENTS

The author expresses gratitude to the Department of Urban and Regional Planning at Rajshahi University of Engineering and Technology (RUET) for their assistance during the data collection phase and their ongoing support throughout the research process. Their contributions were instrumental in ensuring the successful completion of this chapter. The authors also extend their appreciation to the Bangladesh Meteorological Department (BMD), the United States Geological Survey (USGS), and the Survey of Bangladesh for their assistance in supplying the required data for this study at no cost. The data provided by these organizations were crucial in conducting the research and verifying the results. The authors are grateful for their cooperation and support throughout the study.

DATA AVAILABILITY

The datasets that were created and analyzed during this study are available upon request to the corresponding author. To ensure transparency and reproducibility, the corresponding author will respond to requests for the data in a prompt manner. Making the data available to interested parties can facilitate scientific progress and encourage other researchers to expand on the conclusions of this research.

REFERENCES

Ahmed, B., Kamruzzaman, M. D., Zhu, X., Rahman, M., and Choi, K. (2013). Simulating land cover changes and their impacts on land surface temperature in Dhaka, Bangladesh. *Remote Sensing*, 5(11), 5969–5998.

BBS. (2011). *District Statistic*. Bangladesh Bureau of Statistics. The Government of People's Republic of Bangladesh.

Brändle, J. M., Langendijk, G., Peter, S., Brunner, S. H., and Huber, R. (2015). Sensitivity analysis of a land-use change model with and without agents to assess land abandonment and long-term re-forestation in a Swiss mountain region. *Land*, 4(2), 475–512.

Buo, I., Sagris, V., Burdun, I., and Uuemaa, E. (2021). Estimating the expansion of urban areas and urban heat islands (UHI) in Ghana: A case study. *Natural Hazards*, 105(2), 1299–1321. https://doi.org/10.1007/s11069-020-04355-4.

Chavez, P. S. (1996). Image-based atmospheric corrections-revisited and improved. *Photogrammetric Engineering and Remote Sensing*, 62(9), 1025–1035.

Dewan, A., Kiselev, G., and Botje, D. (2021). Diurnal and seasonal trends and associated determinants of surface urban heat islands in large Bangladesh cities. *Applied Geography*, 135, 102533.

Dey, N. N., Al Rakib, A., Kafy, A. A., and Raikwar, V. (2021). Geospatial modelling of changes in land use/land cover dynamics using Multi-layer perception Markov chain model in Rajshahi City, Bangladesh. *Environmental Challenges*, 4, 100148.

dos Santos, R. S. (2020). Estimating spatio-temporal air temperature in London (UK) using machine learning and earth observation satellite data. *International Journal of Applied Earth Observation and Geoinformation*, 88(December 2019), 102066. https://doi.org/10.1016/j.jag.2020.102066.

Dutta, D., Rahman, A., Paul, S. K., and Kundu, A. (2019). Changing pattern of urban landscape and its effect on land surface temperature in and around Delhi. *Environmental Monitoring and Assessment*, 191(9). https://doi.org/10.1007/s10661-019-7645-3.

Farhana, D. K. M., and Mannan, D. K. A. (2018). Socioeconomic impact of regional rural urban migration: A revisit of slum dwellers of Rajshahi City Corporation. Available at SSRN 3098838.

Fathian, F., Prasad, A. D., Dehghan, Z., and Eslamian, S. (2015). Influence of land use/land cover change on land surface temperature using RS and GIS techniques. *International Journal of Hydrology Science and Technology*, 5(3), 195–207.

Ferdous, J., and Rahman, M. T. U. (2018). Temporal dynamics and relationship of land use land cover and land surface temperature in Dhaka, Bangladesh. *Proceedings of the 4th International Conference on Civil Engineering for Sustainable Development (ICCESD 2018)*, 9–11.

Fleiss, J. L., Levin, B., and Paik, M. C. (2004). The measurement of Interrater agreement. In *Statistical Methods for Rates and Proportions*, 598–626. https://doi.org/10.1002/0471445428.ch18.

Fonji, S. F., and Taff, G. N. (2014). Using satellite data to monitor land-use land-cover change in North-eastern Latvia. *SpringerPlus*, 3(61), 1–15. https://doi.org/10.1186/2193-1801-3-61.

Habibie, M. I., Noguchi, R., Shusuke, M., and Ahamed, T. (2021). Land suitability analysis for maize production in Indonesia using satellite remote sensing and GIS-based multicriteria decision support system. *GeoJournal*, 86(2), 777–807.

Hasan, M. H., Sayeeda, N., and Hossain, A. K. M. S. (2017). Developing fire adaptation strategies at community level: A case study of Shreerampur Slum in Rajshahi City Corporation. *International Conference on Planning, Architecture and Civil Engineering. Rajshahi University of Engineering and Technology*, Rajshahi.

Hasan, M. H., Hossain, M. J., Chowdhury, M. A., and Billah, M. (2020). Salinity intrusion in southwest coastal Bangladesh: An insight from land use change. In Haque, A., Chowdhury, A. (Eds.), *Water, Flood Management and Water Security Under a Changing Climate*. Springer, Cham, 125–140. https://doi.org/10.1007/978-3-030-47786-8_8

Hasan, M. H., Chowdhury, M. A., and Wakil, M. A. (2022). Community engagement and public education in northwestern part of Bangladesh: A study regarding heritage conservation. *Heliyon*, 8(3), e09005.

Hasan, M., Newton, I. H., Chowdhury, M. A., Esha, A. A., Razzaque, S., and Hossain, M. J. (2023). Land use land cover change and related drivers have livelihood consequences in coastal Bangladesh. *Earth Systems and Environment*, 7, 1–19.

Hellings, A., and Rienow, A. (2021). Mapping land surface temperature developments in functional urban areas across europe. *Remote Sensing*, 13(11). https://doi.org/10.3390/rs13112111.

Hinkle, D. E., Wiersma, W., and Jurs, S. G. (2003). *Applied Statistics for the Behavioral Sciences*. Houghton Mifflin, Boston.

Hoque, M. A. A., Pradhan, B., and Ahmed, N. (2020). Assessing drought vulnerability using geospatial techniques in northwestern part of Bangladesh. *Science of the Total Environment*, 705, 135957. https://doi.org/10.1016/j.scitotenv.2019.135957.

Hua, A. K., and Ping, O. W. (2018). The influence of land-use/land-cover changes on land surface temperature: A case study of Kuala Lumpur metropolitan city. *European Journal of Remote Sensing*, 51(1), 1049–1069. https://doi.org/10.1080/22797254.2018.1542976.

Imran, H. M., Hossain, A., Islam, A. K. M. S., Rahman, A., Bhuiyan, M. A. E., Paul, S., and Alam, A. (2021). Impact of land cover changes on land surface temperature and human thermal comfort in Dhaka city of Bangladesh. *Earth Systems and Environment*, 5, 1–27. https://doi.org/10.1007/s41748-021-00243-4

Islam, W., and Sarker, S. C. (2016). Monitoring the changing pattern of land use in the Rangpur City corporation using remote sensing and GIS. *Journal of Geographic Information System*, 8(4), 537–545. https://doi.org/10.4236/jgis.2016.84045.

Islam, G. M. T., Islam, A. S., Shopan, A. A., Rahman, M. M., Lázár, A. N., and Mukhopadhyay, A. (2015). Implications of agricultural land use change to ecosystem services in the Ganges delta. *Journal of Environmental Management*, 161, 443–452. https://doi.org/10.1016/j.jenvman.2014.11.018.

Islam, K., Jashimuddin, M., Nath, B., and Nath, T. K. (2018). Land use classification and change detection by using multi-temporal remotely sensed imagery: The case of Chunati wildlife sanctuary, Bangladesh. *The Egyptian Journal of Remote Sensing and Space Science*, 21(1), 37–47. https://doi.org/10.1016/j.ejrs.2016.12.005.

Jain, S., Roy, S. B., Panda, J., and Rath, S. S. (2021). Modeling of land-use and land-cover change impact on summertime near-surface temperature variability over the Delhi–Mumbai Industrial Corridor. *Modeling Earth Systems and Environment*, 7(2), 1309–1319. https://doi.org/10.1007/s40808-020-00959-8.

John, J., Bindu, G., Srimuruganandam, B., Wadhwa, A., and Rajan, P. (2020). Land use/land cover and land surface temperature analysis in Wayanad district, India, using satellite imagery. *Annals of GIS*, 26(4), 343–360.

Kafy, A. A., Al Faisal, A., Sikdar, S., Hasan, M., Rahman, M., Khan, M. H., and Islam, R. (2020). Impact of LULC changes on LST in Rajshahi district of Bangladesh: A remote sensing approach. *Journal of Geographical Studies*, 3, 11–23.

Kafy, A. A., Naim, N. H., Khan, M. H. H., Islam, M. A., Al Rakib, A., Al-Faisal, A., and Sarker, M. H. S. (2021a). Prediction of urban expansion and identifying its impacts on the degradation of agricultural land: A machine learning-based remote-sensing approach in Rajshahi, Bangladesh. In Singh R. (Ed), *Re-envisioning Remote Sensing Applications*. CRC Press, Boca Raton, 85–106.

Kafy, A. A., Al Faisal, A., Al Rakib, A., Roy, S., Ferdousi, J., Raikwar, V., Kona, M. A., and Al Fatin, S. M. A. (2021b). Predicting changes in land use/land cover and seasonal land surface temperature using multi-temporal landsat images in the northwest region of Bangladesh. *Heliyon*, 7(7), e07623. https://doi.org/10.1016/j.heliyon.2021.e07623.

Kafy, A. A., Rahman, A. N. M. F., Al Rakib, A., Akter, K. S., Raikwar, V., Jahir, D. M. A., Ferdousi, J., and Kona, M. A. (2021c). Assessment and prediction of seasonal land surface temperature change using multi-temporal Landsat images and their impacts on agricultural yields in Rajshahi, Bangladesh. *Environmental Challenges*, 4, 100147.

Kafy, A. A., Al Rakib, A., Akter, K. S., Rahaman, Z. A., Faisal, A.-A., Mallik, S., Nasher, N. M. R., Hossain, M. I., and Ali, M. Y. (2021d). Monitoring the effects of vegetation cover losses on land surface temperature dynamics using geospatial approach in Rajshahi city, Bangladesh. *Environmental Challenges*, 4, 100187.

Lai, L. W., and Cheng, W. L. (2010). Urban heat island and air pollution-an emerging role for hospital respiratory admissions in an urban area. *Journal of Environmental Health*, 72(6), 32–35.

Liu, F., Hou, H., and Murayama, Y. (2021). Spatial interconnections of land surface temperatures with land cover/use: A case study of Tokyo. *Remote Sensing*, 13(4), 1–26. https://doi.org/10.3390/rs13040610.

López-Serrano, P. M., Corral-Rivas, J. J., Díaz-Varela, R. A., Álvarez-González, J. G., and López-Sánchez, C. A. (2016). Evaluation of radiometric and atmospheric correction algorithms for aboveground forest biomass estimation using Landsat 5 TM data. *Remote Sensing*, 8(5), 369.

Lu, D., Mausel, P., Brondízio, E., and Moran, E. (2004). Change detection techniques. *International Journal of Remote Sensing*, 25(12), 2365–2401. https://doi.org/10.1080/0143116031000139863.

Makvandi, M., Li, B., Elsadek, M., Khodabakhshi, Z., and Ahmadi, M. (2019). The interactive impact of building diversity on the thermal balance and micro-climate change under the influence of rapid urbanization. *Sustainability*, 11(6), 1–20. https://doi.org/10.3390/su11061662.

Mas, J. F. (1999). Monitoring land-cover changes: A comparison of change detection techniques. *International Journal of Remote Sensing*, 20, 139–152. https://doi.org/10.1080/014311699213659.

Mim, M. A., and Zamil, K. M. S. (2020). GIS-based surface water changing analysis in rajshahi city corporation area using ensemble classifier. *Proceedings of International Joint Conference on Computational Intelligence*, 39–47.

Mirza, M. M. Q. (2011). Climate change, flooding in South Asia and implications. *Regional Environmental Change*, 11(1), 95–107.

Mustafa, E. K., Abd El-Hamid, H. T., and Tarawally, M. (2021). Spatial and temporal monitoring of drought based on land surface temperature, Freetown City, Sierra Leone, West Africa. *Arabian Journal of Geosciences*, 14(11). https://doi.org/10.1007/s12517-021-07187-z.

NASA. (2015). *Landsat 8 Data User Handbook*. National Aeronautics and Space Administration.

Pal, S., and Ziaul, S. K. (2017). Detection of land use and land cover change and land surface temperature in English Bazar urban centre. *The Egyptian Journal of Remote Sensing and Space Science*, 20(1), 125–145.

Rahaman, M. A., Hossain, M. I., Kamal, A., and Chowdhury, A. M. (2021). Climate-induced displacement and human migration landscape in Bangladesh. In *Handbook of Climate Change Management*. https://doi.org/10.1007/978-3-030-22759-3_255-1.

Rahman, M. M. (2010). Factors of economic transformation in sub-urban areas of Rajshahi City, Bangladesh. *Journal of Life and Earth Science*, 5, 47–55.

Raja, D. R. (2012). GIS-based spatial simulation of impacts of urban development on changing both land cover area and land surface temperature in Dhaka city. Dissertation, Bangladesh University of Engineering and Technology, Bangladesh.

Roy, B., Bari, E., Nipa, N. J., and Ani, S. A. (2021). Comparison of temporal changes in urban settlements and land surface temperature in Rangpur and Gazipur Sadar, Bangladesh after the establishment of city corporation. *Remote Sensing Applications: Society and Environment*, 23, 100587.

Rwanga, S. S., and Ndambuki, J. M. (2017). Accuracy assessment of land use/land cover classification using remote sensing and GIS. *International Journal of Geosciences*, 8(4), 611.

Siddique, M. A., Dongyun, L., Li, P., Rasool, U., Khan, T. U., Farooqi, T. J. A., Wang, L., Fan, B., and Rasool, M. A. (2020). Assessment and simulation of land use and land cover change impacts on the land surface temperature of Chaoyang District in Beijing, China. *PeerJ*, 2020(3), 1–26. https://doi.org/10.7717/peerj.9115.

Souza, D. O. de, Alvalá, R. C. dos S., and Nascimento, M. G. do. (2016). Urbanization effects on the micro-climate of Manaus: A modeling study. *Atmospheric Research*, 167(January), 237–248. https://doi.org/10.1016/j.atmosres.2015.08.016.

Teillet, P. M. (1986). Image correction for radiometric effects in remote sensing. *International Journal of Remote Sensing*, 7, 1637–1651. https://doi.org/10.1080/01431168608948958.

Turker, M., and Asik, O. (2002). Detecting land use changes at the urban fringe from remotely sensed images in Ankara, Turkey. *Geocarto International*, 17, 47–52. https://doi.org/10.1080/10106040208542243.

WB. (2013). *Warming Climate to Hit Bangladesh Hard with Sea Level Rise, More Floods and Cyclones*. World Bank, Washington, DC.

Weng, Q., Lu, D., and Schubring, J. (2004). Estimation of land surface temperature–vegetation abundance relationship for urban heat island studies. *Remote Sensing of Environment*, 89(4), 467–483.

Zhang, X. Q. (2016). The trends, promises and challenges of urbanisation in the world. *Habitat International*, 54(November 2015), 241–252. https://doi.org/10.1016/j.habitatint.2015.11.018.